

Electronic Supporting Information (ESI) for

A New High Voltage *Alluaudite* Sodium Battery Insertion Material

Pubali Barman^a, Pawan Kumar Jha^a, Anshuman Chaupatnaik^a, K. Jayanthi^{b,c}, Rayavarapu Prasada Rao^d, Gopalakrishnan Sai Gautam^e, Sylvain Franger^f, Alexandra Navrotsky^b, and Prabeer Barpanda^{a,g,h*}

^aFaraday Materials Laboratory (FaMaL), Materials Research Center, Indian Institute of Science, Bangalore 560012, India.

^bSchool of Molecular Sciences and Navrotsky Eyring Center for Materials of the Universe, Arizona State University, Tempe, Arizona 85287, United States.

^cChemical Sciences Division, Oak Ridge National Laboratory, Oak Ridge, Tennessee 37831, United States.

^dDepartment of Mechanical Engineering, National University of Singapore, 117575 Singapore.

^eDepartment of Materials Engineering, Indian Institute of Science, Bangalore 560012, India.

^fInstitut de Chimie Moléculaire et des Matériaux d'Orsay (ICMMO-CNRS), UMR 8182 CNRS-Université Paris-Saclay, 410 Rue du Doyen Georges Poitou, 91405, Orsay, France.

^gHelmholtz Institute Ulm (HIU), Electrochemical Energy Storage, Ulm 89081, Germany.

^hInstitute of Nanotechnology, Karlsruhe Institute of Technology (KIT), Karlsruhe 76021, Germany.

*Corresponding Author E-mail: prabeer@iisc.ac.in

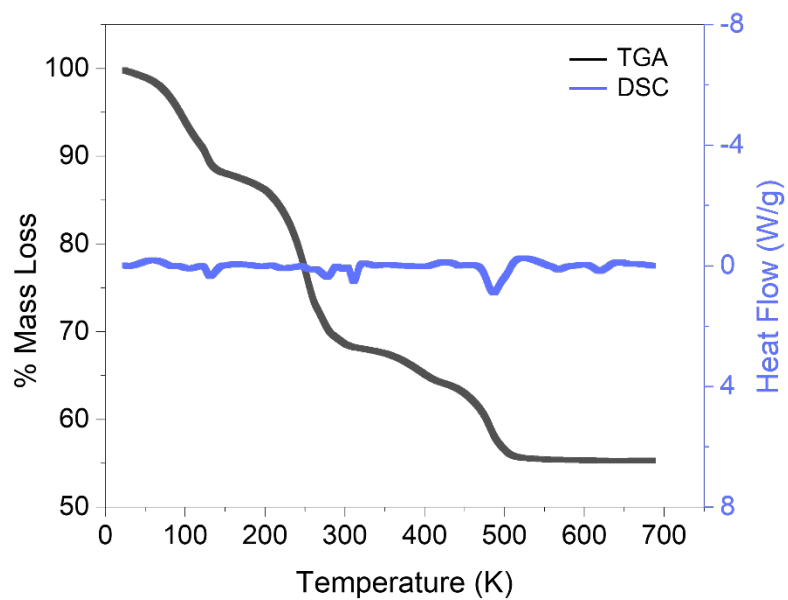


Fig. S1: Thermal analysis of the precursor mixture. The blue solid line indicates differential scanning calorimetry (DSC) curve showing several endothermic peaks, and the black line refers to the thermogravimetric analysis showing the weight loss as a function of temperature.

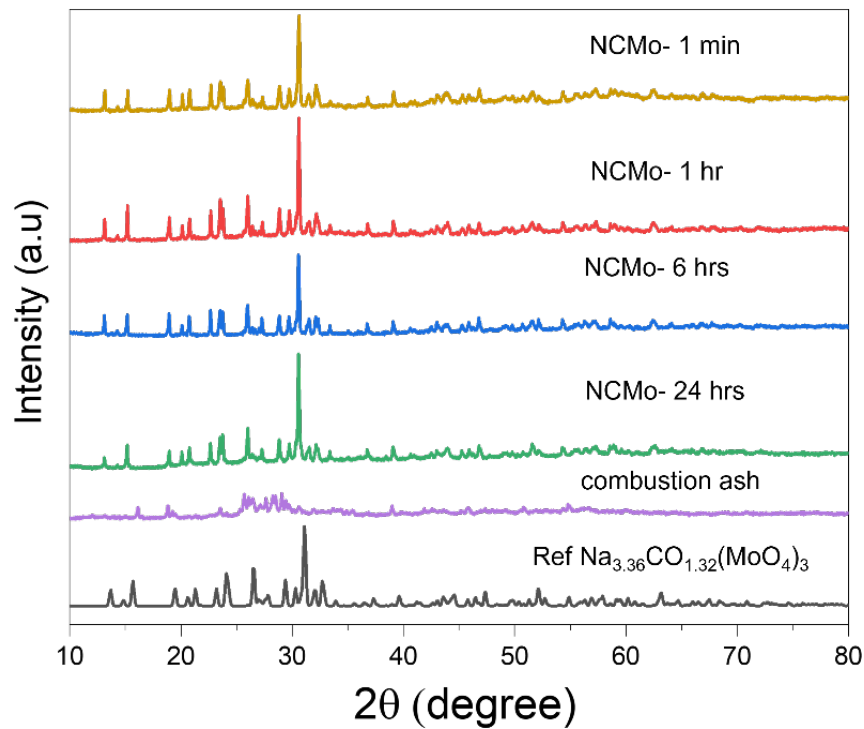


Fig. S2: Comparative PXRD patterns of $\text{Na}_{3.36}\text{CO}_{1.32}(\text{MoO}_4)_3$ (NCMo) product phases obtained after annealing for different duration starting from 24 hours to 1 minute. The PXRD patterns of combustion ash (intermediate product) and ICSD reference data are shown.

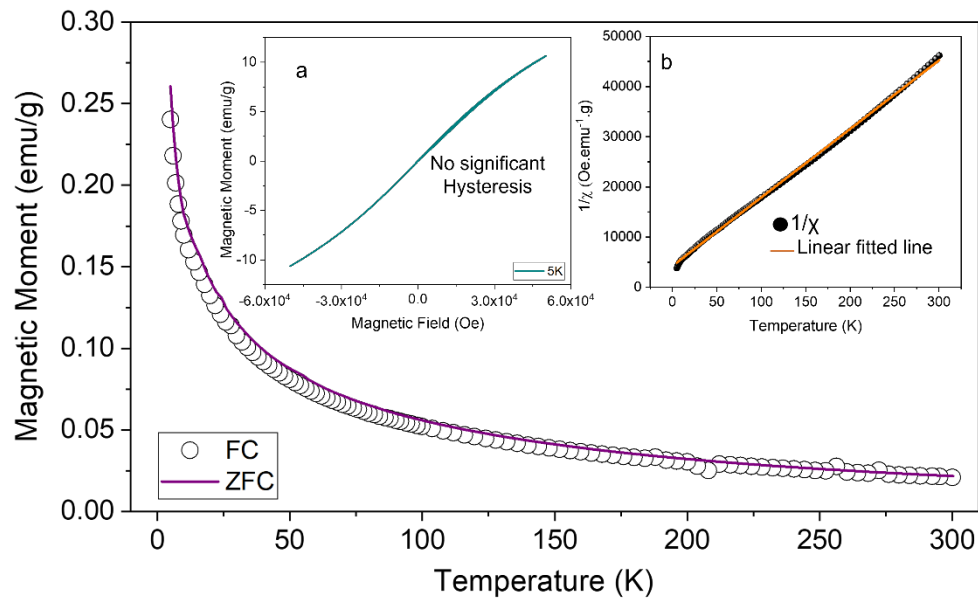


Fig. S3: Temperature-dependent magnetization curve of *alluaudite*-Na_{3.36}Co_{1.32}(MoO₄)₃ measured in zero-field cooled (ZFC, purple line) and field-cooled (FC, black open balls) modes at 1000 Oe between 5 K to 300 K. Magnetization (M vs H) curve (inset a) of the target compound recorded at 5 K shows no signature of ferromagnetic hysteresis. The inverse magnetic susceptibility (black circles and orange line) vs temperature plot reveals a deviation at \sim 10 K can be related to some local ordering.

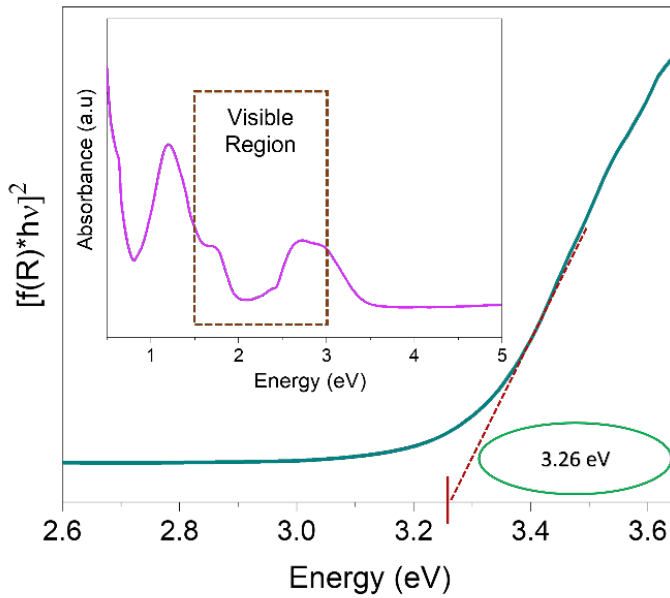


Fig. S4: Optical band gap for the alluaudite material using Kubelka-Munk functions ($n=2$) applied to UV-visible-NIR spectra. The inset image is showing the UV-visible absorption spectra involving different d-d transitions with two distinct peaks in the visible region.

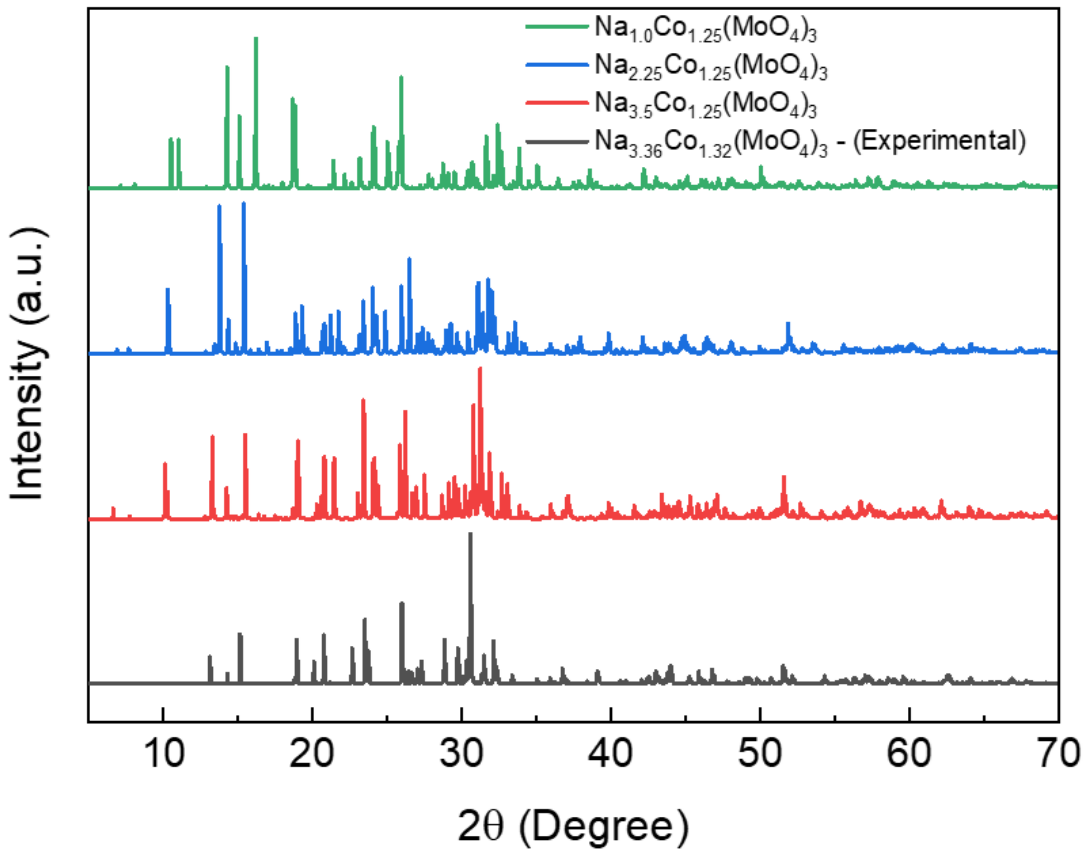


Fig. S5: Simulated XRD patterns of SCAN+*U* relaxed structures for $\text{Na}_{3.5}\text{Co}_{1.25}(\text{MoO}_4)_3$ at different states of (de)sodiation along with the experimental .cif file.

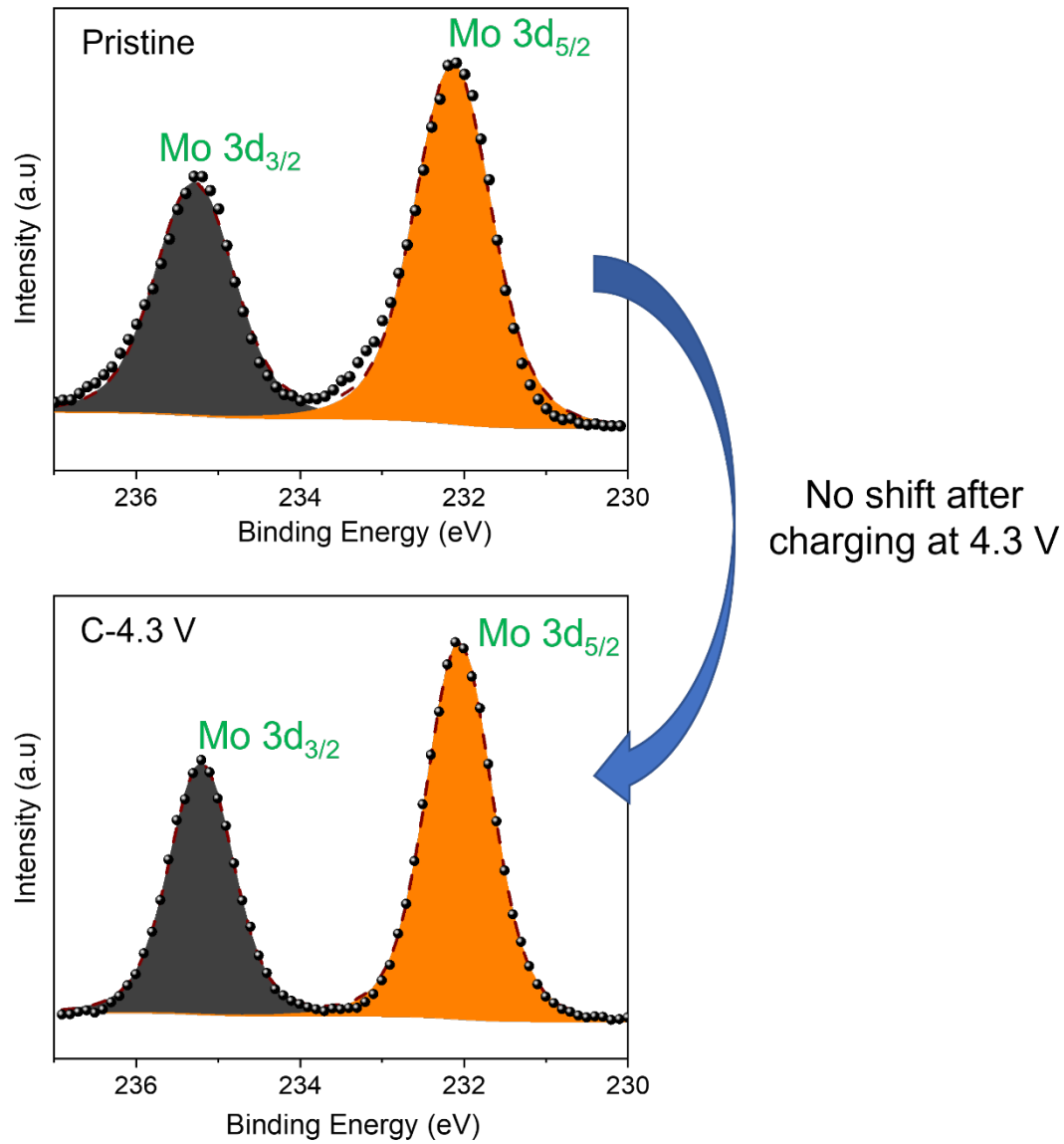


Fig. S6: High-resolution XPS spectra of Mo 3d orbital at its pristine and charged (4.3 V) state which shows no shift in the Mo peak indicating the absence of Mo-redox within the voltage range of 3.0 to 4.3 V.

Table S1. Crystallographic parameters determined by Rietveld refinement of high-resolution XRD data ($\lambda = 1.5418 \text{ \AA}$) of combustion synthesized sample.

Formula [molecular weight]	Na _{3.36} Co _{1.32} (MoO ₄) ₃ [635.16 g/mol]
Crystal system	Monoclinic
Space group	C2/c (#15)
Unit cell parameter (Å)	$a = 12.63174(35)$, $b = 13.49553(33)$, $c = 7.12597(16)$ $\beta = 112.1460^\circ$, $Z = 4$
Unit cell volume (Å ³)	1125.160
Theoretical density (g cm ⁻³)	3.75
Goodness of fit value	$\chi^2 = 4.775\%$

	Site	x	y	z	Occupancy	U _{iso}
Mo1	4e	0.0	0.78720 (7)	0.25	1	0.00293 (6)
Mo2	8f	0.23145 (3)	0.60593 (7)	0.12464 (5)	1	0.00692 (5)
Co1	8f	0.29072 (7)	0.83724 (0)	0.36969 (6)	0.66003 (1)	0.00351 (9)
Na1	8f	0.28808 (1)	0.84434 (4)	0.38740 (8)	0.33997 (1)	0.00351 (9)
Na2	4a	0.0	0.0	0.0	1.0	0.05254 (5)
Na3	4e	0.0	0.23573 (2)	0.25	0.68591 (5)	0.00141 (2)
Na4	4e	0.0	0.50558 (0)	0.25	1.0	0.05614 (1)
O1	8f	0.16621 (5)	0.33438 (0)	0.38586 (8)	1.0	0.05560 (3)
O2	8f	0.12066 (8)	0.08834 (4)	0.31052 (9)	1.0	0.06204 (3)
O3	8f	0.38426 (9)	0.38436 (1)	0.25855 (9)	1.0	0.10050 (4)
O4	8f	0.28004 (7)	0.17323 (9)	0.16689 (3)	1.0	0.05156 (4)
O5	8f	0.02588 (4)	0.70924 (3)	0.47829 (5)	1.0	0.03189 (3)
O6	8f	0.14525 (7)	0.49714 (0)	0.10549 (8)	1.0	0.12520 (5)

Table S2. SCAN+*U* predicted change in on-site magnetic moment of Co and Mo at various (de)Sodiation states.

Elements	$\text{Na}_{3.25}\text{Co}_{1.25}(\text{MoO}_4)_3$	$\text{Na}_{2.25}\text{Co}_{1.25}(\text{MoO}_4)_3$	$\text{NaCo}_{1.25}(\text{MoO}_4)_3$
Co1	2.755	-0.01	-0.046
Co2	2.754	0.028	-1.886
Co3	2.766	0.001	0.832
Co4	-2.746	0.002	-0.008
Co5	-2.756	0.006	-0.759
Mo1	0.009	-0.005	-0.012
Mo2	0.000	-0.005	-0.005
Mo3	0.000	0.003	0.045
Mo4	0.011	-0.006	0.001
Mo5	0.012	0.004	-0.056
Mo6	-0.009	0.004	-0.066
Mo7	-0.015	0.003	0.003
Mo8	-0.011	-0.004	-0.014
Mo9	0.010	-0.005	-0.015
Mo10	0.019	-0.003	-0.01
Mo11	0.012	0.007	0.002
Mo12	0.015	0.000	-0.001

Table S3. SCAN+*U*-calculated Co-O bond lengths at various (de)sodiated states.

Na_{3.25}Co_{1.25}(MoO₄)₃	Na_{2.25}Co_{1.25}(MoO₄)₃	NaCo_{1.25}(MoO₄)₃
(Co1-O6) = 2.07548(0) Å	(Co1-O6) = 1.90138(0) Å	(Co1-O6) = 1.88378(0) Å
(Co1-O22) = 1.98881(0) Å	(Co1-O22) = 1.84718(0) Å	(Co1-O46) = 1.92669(0) Å
(Co1-O46) = 2.10163(0) Å	(Co1-O46) = 1.93627(0) Å	(Co1-O30) = 1.91394(0) Å
(Co1-O30) = 2.32373(0) Å	(Co1-O30) = 2.03366(0) Å	(Co1-O39) = 1.85019(0) Å
(Co1-O39) = 1.98847(0) Å	(Co1-O39) = 1.90255(0) Å	(Co1-O22) = 1.86683(0) Å
(Co1-O25) = 2.12800(0) Å	(Co1-O25) = 1.96698(0) Å	(Co1-O25) = 1.93681(0) Å
(Co2-O31) = 2.09593(0) Å	(Co2-O31) = 2.00504(0) Å	(Co2-O31) = 1.90910(0) Å
(Co2-O44) = 2.21882(0) Å	(Co2-O20) = 1.93818(0) Å	(Co2-O20) = 1.89484(0) Å
(Co2-O33) = 2.04159(0) Å	(Co2-O44) = 2.02020(0) Å	(Co2-O44) = 1.94732(0) Å
(Co2-O20) = 2.04404(0) Å	(Co2-O33) = 1.92504(0) Å	(Co2-O4) = 1.88517(0) Å
(Co2-O28) = 2.10193(0) Å	(Co2-O28) = 1.90710(0) Å	(Co2-O33) = 1.81930(0) Å
(Co2-O4) = 2.12668(0) Å	(Co2-O4) = 2.03164(0) Å	
(Co3-O30) = 2.11728(0) Å	(Co3-O30) = 1.99564(0) Å	(Co3-O30) = 1.87016(0) Å
(Co3-O36) = 2.01055(0) Å	(Co3-O36) = 1.87131(0) Å	(Co3-O36) = 1.79247(0) Å
(Co3-O41) = 2.08277(0) Å	(Co3-O41) = 1.89442(0) Å	(Co3-O41) = 1.86925(0) Å
(Co3-O25) = 2.16523(0) Å	(Co3-O17) = 1.88442(0) Å	(Co3-O25) = 1.87062(0) Å
(Co3-O17) = 1.98595(0) Å	(Co3-O25) = 1.95424(0) Å	(Co3-O17) = 1.88504(0) Å
(Co3-O1) = 2.09645(0) Å	(Co3-O1) = 1.95056(0) Å	(Co3-O1) = 1.87346(0) Å
(Co4-O2) = 2.09331(0) Å	(Co4-O2) = 1.92448(0) Å	(Co4-O2) = 1.87249(0) Å
(Co4-O18) = 2.07090(0) Å	(Co4-O18) = 2.00504(0) Å	(Co4-O18) = 1.95733(0) Å
(Co4-O26) = 2.13277(0) Å	(Co4-O26) = 1.90780(0) Å	(Co4-O26) = 1.89281(0) Å
(Co4-O42) = 2.05823(0) Å	(Co4-O42) = 1.83830(0) Å	(Co4-O42) = 1.86885(0) Å
(Co4-O35) = 2.04460(0) Å	(Co4-O35) = 1.92512(0) Å	(Co4-O35) = 1.92475(0) Å
(Co4-O29) = 2.11637(0) Å	(Co4-O29) = 1.96590(0) Å	(Co4-O29) = 1.91426(0) Å
(Co5-O26) = 2.10865(0) Å	(Co5-O26) = 1.92712(0) Å	(Co5-O26) = 1.89212(0) Å
(Co5-O40) = 2.06997(0) Å	(Co5-O40) = 1.94871(0) Å	(Co5-O40) = 1.77595(0) Å
(Co5-O29) = 2.18669(0) Å	(Co5-O29) = 1.92964(0) Å	(Co5-O29) = 1.82762(0) Å
(Co5-O45) = 2.06089(0) Å	(Co5-O45) = 1.85419(0) Å	(Co5-O5) = 1.87778(0) Å
(Co5-O21) = 2.01887(0) Å	(Co5-O21) = 1.90379(0) Å	(Co5-O45) = 1.86518(0) Å
(Co5-O5) = 2.06190(0) Å	(Co5-O5) = 1.90872(0) Å	(Co5-O21) = 1.90955(0) Å